Statistical tensors for the analysis of γ-ray emission from a non-axially-symmetric nuclear ensemble

G. J. Bowden,* I. A. Campbell,† N. Nambudripad, and N. J. Stone

Mullard Cryomagnetic Laboratory, Clarendon Laboratory, University of Oxford, Oxford, OX1 3PU, United Kingdom

(Received 14 August 1978)

A tabulation of statistical tensors $\rho_q^\lambda(I)$ for the analysis of γ-ray emission from a non-axially-symmetric nuclear ensemble

$$H = AI_z + P\{-\tfrac{1}{2}[I_z^2 - \tfrac{1}{3}I(I+1)] + \tfrac{1}{2}(I_+^2 + I_-^2)\}$$

has been prepared. The tables cover all values of the magnetic and quadrupole hyperfine parameters A and P, for $1 \leq I \leq 8$. Explicit rotation matrices are also given which enable the tabulated statistical tensors to be transformed into those appropriate to other frames of reference. Special attention is given to off-diagonal tensors $\rho_q^\lambda(I)$, $q \neq 0$, and it is suggested that statistical-tensor diagrams $\rho_2^2(I)$ vs $\rho_0^2(I)$, etc., are a useful way of presenting nuclear-orientation data.

I. INTRODUCTION

In 1959 Samoilov[1] discovered that many elements, dissolved in ferromagnetic metals, experience magnetic hyperfine interactions of sufficient magnitude to produce anisotropy in their γ-ray angular distributions at temperatures in the 10-mK range. Since that time the vast majority of nuclear-orientation experiments have been carried out on dilute magnetic alloys in which the nuclear hyperfine Hamiltonian possesses simple axial symmetry about the direction of an applied magnetic field. Even the earlier work on self-cooling dielectric crystals of transition-metal, rare-earth, and actinide elements exploited uniaxial crystals, with their attendant simplicity in the angular distribution of the emitted decay products.

However, in general, the angular distribution of decay products from systems lacking axial symmetry can be used to extract information concerning the strengths and relative orientations of the interactions to which the oriented nuclei are subject. Examples of such systems are (i) the magnetic-field properties of antiferromagnetic and more complex spin structures; (ii) Kondo-state systems in noncubic materials and; (iii) singlet-ground-state systems with nonvanishing quadrupole interactions. Such investigations of course require single crystals *per se*. Motivation for the present work stems from recent experiments on the Van Vleck enhanced nuclear antiferromagnet $HoVO_4$. This compound affords an example of the most commonly encountered nonaxial system in which the magnetic hyperfine field makes a right angle with the axis of an axially symmetric nuclear quadrupole interaction. Analysis of the angular distributions from systems with an n-fold symmetry axis ($n < \infty$) is given in Paper II (following article, this issue) and is relevant to various types of ordered spin systems.

For the mixed magnetic plus electric interaction described above, the nuclear hyperfine Hamiltonian may be written in the form

$$H = AI_z + P\{-\tfrac{1}{2}[I_z^2 - \tfrac{1}{3}I(I+1)] + \tfrac{1}{2}(I_+^2 + I_-^2)\} \quad , \quad (1)$$

where

$$A = g\mu_N B \quad (2)$$

and

$$P = 3e^2Qq/4I(2I-1) \quad , \quad (3)$$

which reveals that $I_z = m$ is not a good quantum number. As a result, the standard treatment of the γ-ray emission problem, detailed, for example, by Steffen and Frauenfelder[2] and Steffen and Adler,[3] must fail. In particular, statistical tensors $\rho_q^\lambda(I_i)$ with $q \neq 0$ do not vanish identically and their presence gives rise to azimuthal variations $\cos(q\phi)$ in the angular distribution function $W(\theta,\phi)$.

In order to facilitate the analysis of γ-ray emission from nuclear ensembles described by Eq. (1), tables of statistical tensors $\rho_0^2(I)$, $\rho_2^2(I)$, $\rho_0^4(I)$, $\rho_2^4(I)$, and $\rho_4^4(I)$ have been prepared. These tables cover all the values of the magnetic and quadrupole parameters A and P, for $1 \leq I \leq 8$. The method adopted for the computation of the statistical tensors is outlined in Sec. III, and the system underlying the presentation of the tables is explained in Sec. IV. In Sec. V, the symmetry properties of the $\rho_q^\lambda(I)$ are used to derive rotation matrices, which allow the tabulated statistical

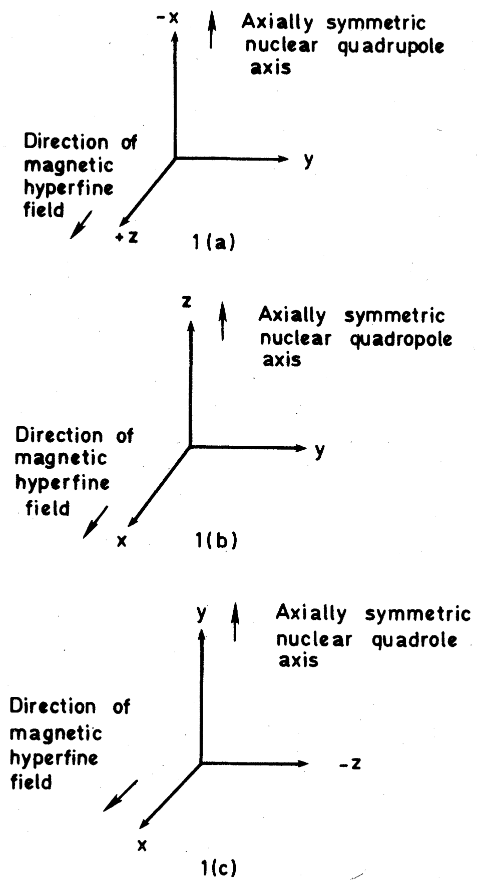

FIG. 1. Relationships between the various right-handed frames of reference used in this paper.

tensors to be transformed into those appropriate to the three frames of reference shown in Figs. 1(a)–1(c). Finally, in Sec. VI, it is argued that statistical tensor-diagrams $\rho_2^2(I)$ vs $\rho_0^2(I)$, etc., are a useful way of presenting nuclear-orientation data, particularly when nuclear spin-flop transitions are likely to occur.

II. DEFINITIONS AND SYMMETRY CONSIDERATIONS

Following Steffen and Alder,[3] the angular distribution function for γ rays may be written

$$W(\theta,\phi)=\frac{\delta\Omega}{2\pi^{1/2}}\sum_{\lambda,q}(2I_i+1)^{1/2}(2\lambda+1)^{-1/2}\times A_\lambda(\gamma)\rho_q^\lambda(I_i)\,Y_{\lambda q}{}^*(\theta,\phi)\ , \qquad (4)$$

where (i) I_i is the spin of the initial nuclear state; (ii) λ is the rank of the multipole emission (for most practical purposes we have $\lambda=2$ and 4 only); (iii) $A_\lambda(\gamma)$ is a nuclear parameter which depends, in part, on the mixing ratio δ for $M1$ and $E2$ transitions; (iv) $\rho_q^\lambda(I_i)$ is a statistical tensor or state multipole[4,5] which describes the orientation of the nuclear ensemble and; (v) $Y_{\lambda q}(\theta,\phi)$ is a spherical harmonic of rank λ. For convenience a brief list of spherical harmonics may be found in Table I. The statistical tensors $\rho_q^\lambda(I_i)$ may be calculated via the formula

$$\rho_q^\lambda(I_i)=\sum_m(-)^{I_i+m}\langle I_i -m\; I_i m'|\lambda q\rangle\,\langle I_i m|\,\underline{\rho}\,|I_i m'\rangle\ , \qquad (5)$$

where $\underline{\rho}$ the density matrix, is given by

$$\underline{\rho}=e^{-\beta H}/\mathrm{Tr}(e^{-\beta H}) \qquad (6)$$

for a system in thermal equilibrium, and $\langle I_i -m\; I_i m'|\lambda q\rangle$ is a Clebsch-Gordan coefficient, defined, for example, by Edmonds.[6]

The usefulness of the statistical tensor formulation of the γ-ray emission problem lies in their transformation properties under spatial rotations. Following a rotation of the co-ordinate system through the Euler angles α, β, and γ, the statistical tensors $(\rho_q^\lambda)'$ referred to the new primed axes are related to those referred to the old axes via the equation

$$\rho_q^{\lambda\prime}=\sum_{q''}\mathfrak{D}^{\lambda}_{q''q}(\alpha,\beta,\gamma)\,\rho^\lambda_{q''}\ , \qquad (7)$$

where the $\mathfrak{D}^{\lambda}_{q''q}(\alpha,\beta,\gamma)$ are the well-known rotation matrices.[6]

Thus, the statistical tensors ρ_q^λ form a complete set, transforming as a tensor operator of rank λ.

One further symmetry relation which we shall find useful is

$$\rho_q^{\lambda *}=(-)^q\rho^\lambda_{-q}\ . \qquad (8)$$

This identity is easily proved on making use of the symmetry properties of Clebsch-Gordan coefficients, together with the Hermitian character of the density matrix $\underline{\rho}$. As a result, Eq. (4) may be recast in the form

$$W(\theta,\phi)=\frac{\delta\Omega}{2\pi^{1/2}}\sum_{\lambda\,\mathrm{even}}(2I_i+1)^{1/2}(2\lambda+1)^{-1/2}A_\lambda(\gamma)\times\left\{\rho_0^\lambda(I_i)\,Y_{\lambda 0}(\theta,\phi)+\sum_{q>0}\left[\rho_q^\lambda(I_i)\,Y^*_{\lambda q}(\theta,\phi)+(-)^q\rho^{\lambda *}_{+q}(I_i)\,Y_{\lambda -q}(\theta,\phi)\right]\right\}\ , \qquad (9)$$

which reveals that the angular distribution function is completely determined by statistical tensors $\rho_q^\lambda(I_i)$ with $q \geqslant 0$. For the Hamiltonian described by Eq. (1) therefore, we write

$$W(\theta,\phi)=\frac{\delta\Omega}{4\pi}\Bigg\{1+A_2(\gamma)(2I_i+1)^{1/2}[\rho_0^2\,\tfrac{1}{2}(3\cos^2\theta-1)+\rho_2^2(\tfrac{3}{2})^{1/2}(1-\cos^2\theta)\cos2\phi]$$
$$+A_4(\gamma)\Bigg[\rho_0^4\,\tfrac{1}{8}(35\cos^4\theta-30\cos^2\theta+3)+\rho_2^4\,\tfrac{1}{2}(\tfrac{5}{2})^{1/2}(1-\cos^2\theta)(7\cos^2\theta-1)\cos2\phi$$
$$+\rho_4^4\frac{35^{1/2}}{4(2)^{1/2}}(1-\cos^2\theta)^2\cos4\phi\Bigg]\Bigg\}\ , \quad (10)$$

where the series has been terminated at $\lambda=4$. Note that for arbitrary angles θ between the magnetic hyperfine field $\vec{B}$ and the electric quadrupole axis, statistical tensors with odd q may also be nonzero.

III. COMPUTATION OF STATISTICAL TENSORS

From the definition of the statistical tensors given in Eq. (5), it is clear that matrix elements $\langle I_i m|\underline{\rho}|I_i m'\rangle$ are required, where m' is not necessarily equal to m. This can be achieved with the aid of a diagonalization routine which supplies not only the energy eigenvalues E_k, but also the unitary matrix $\underline{U}$, which reduces $\underline{H}$ to diagonal form

$$(\underline{U}^{-1}\underline{H}\underline{U})_{kk'}=(\underline{H_E})_{kk'}=E_k\delta_{kk'}\ . \quad (11)$$

Given $\underline{H_E}$, it is a relatively easy matter to form the density matrix

$$(\underline{\rho_E})_{kk'}=e^{-\beta E_k}/\mathrm{Tr}(e^{-\beta E_k})\delta_{kk'}\ , \quad (12)$$

which can subsequently be used to generate $\underline{\rho}$, in the Zeeman representation, via the back transformation

$$\underline{\rho}=\underline{U}\underline{\rho_E}\underline{U}^{-1}\ . \quad (13)$$

The statistical tensors $\rho_q^\lambda(I_i)$ can then be calculated, with the aid of Eqs. (5) and (13), in conjunction with a Clebsch-Gordan routine.

As noted earlier, statistical tensors with odd q are identically equal to zero, for the Hamiltonian defined by Eq. (1), because the angle between the principal axis of the quadrupole interaction and the magnetic hyperfine field is $\frac{1}{2}\pi$. Consequently, in preparing tables of the $\rho_q^\lambda(I)$, it is only necessary to tabulate (ρ_0^2,ρ_2^2) and $(\rho_0^4,\rho_2^4,\rho_4^4)$, for $M1$ and $E2$ γ-ray transitions. However, because of space limitations only the tables for $I=3, 7$ are appended to this paper.[7]

TABLE I.

	Spherical harmonics for $l=2$ and 4	Legendre polynomials
Definition	$Y_{lm}(\theta,\phi)=i^{m+\lvert m\rvert}\left[\frac{2l+1}{4\pi}\frac{(l-\lvert m\rvert)!}{(l+\lvert m\rvert)!}\right]P_l^{\lvert m\rvert}(\cos\theta)e^{im\phi}$	$P_n^m(x)=(1-x^2)^{\lvert m\rvert/2}\frac{d^{\lvert m\rvert}}{dx^{\lvert m\rvert}}P_n(x)$
$l=2$	$Y_{20}(\theta,\phi)=\left[\frac{5}{4\pi}\right]^{1/2}P_2^0(\cos\theta)$	$P_2^0(\cos\theta)=\frac{1}{2}(3\cos^2\theta-1)$
	$Y_{2\pm2}(\theta,\phi)=\left[\frac{5}{4\pi}\times\frac{1}{4!}\right]^{1/2}P_2^2(\cos\theta)e^{\pm i2\phi}$	$P_2^2(\cos\theta)=3(1-\cos^2\theta)$
$l=4$	$Y_{40}(\theta,\phi)=\left[\frac{9}{4\pi}\right]^{1/2}P_4^0(\cos\theta)$	$P_4^0(\cos\theta)=\frac{1}{8}(35\cos^4\theta-30\cos^2\theta+3)$
	$Y_{4\pm2}(\theta,\phi)=\left[\frac{9}{4\pi}\times\frac{2!}{6!}\right]^{1/2}P_4^2(\cos\theta)e^{\pm i2\phi}$	$P_4^2(\cos\theta)=\frac{15}{2}(1-\cos^2\theta)(7\cos^2\theta-1)$
	$Y_{4\pm4}(\theta,\phi)=\left[\frac{9}{4\pi}\times\frac{1}{8!}\right]^{1/2}P_4^4(\cos\theta)e^{\pm i4\phi}$	$P_4^4(\cos\theta)=105(1-\cos^2\theta)^2$

IV. PRESENTATION OF THE TABLES

In order to tabulate statistical tensors for all values of A and P, it is advantageous to recast the Hamiltonian defined by Eq. (1) into the equivalent form discussed below.

First we rewrite H in the normalized operator form

$$H = A'(I_z/2I) + P'\{-\tfrac{1}{2}[I_z^2 - \tfrac{1}{3}I(I+1)] + \tfrac{1}{2}(I_+^2 + I_-^2)\}/[I^2 - ((\tfrac{1}{4}))] \ , \tag{14}$$

where

$$A' = A \times 2I \ , \tag{15}$$

$$P' = P[I^2 - ((\tfrac{1}{4}))] \ , \tag{16}$$

and $((\frac{1}{4}))$ implies that we have $((\frac{1}{4})) = 0, \frac{1}{4}$ if I is integer, half integer, respectively. Note that the total splitting associated with the normalized Zeeman and quadrupole operators, taken separately, is equal to unity.

Next we recast Eq. (14) in the form

$$H = W'\left\{x(I_z/2I) + (1-x)\{-\tfrac{1}{2}[I_z^2 - \tfrac{1}{3}I(I+1)] + \tfrac{1}{2}(I_+^2 + I_-^2)\}/[I^2 - ((\tfrac{1}{4}))]\right\} \ , \tag{17}$$

where

$$W'x = A' = A \times 2I \ , \tag{18}$$

$$W'(1-x) = P' = P[I^2 - ((\tfrac{1}{4}))] \ . \tag{19}$$

W' is essentially a measure of the strength of the Hamiltonian H, while x determines the ratio of the magnetic to quadrupole parameters, via the equation

$$\frac{A'}{P'} = \frac{x}{1-x} = \frac{A}{P}\frac{2I}{I^2 - ((\frac{1}{4}))} \ . \tag{20}$$

Finally we observe, from an examination of Eqs. (5) and (6), that it is βH rather than H which determines the value of a given statistical tensor. We set therefore

$$\beta H = W\left\{x(I_z/2I) + (1-x)\{-\tfrac{1}{2}[I_z^2 - \tfrac{1}{3}I(I+1)] + \tfrac{1}{2}(I_+^2 + I_-^2)\}\right\}/[I^2 - ((\tfrac{1}{4}))] \ , \tag{21}$$

where

$$W = \beta W' = W'/kT \ . \tag{22}$$

This suggests that tables of statistical tensors $\rho_q^\lambda(I_i)$ are best prepared in the form of a two-dimensional array, spanned by the parameters W and x where, for a given interaction, increasing W corresponds to decreasing temperature. Note that for $x = 0$ (1.0), the tabulated statistical tensors are those for the pure quadrupole (magnetic) interaction, respectively.

Finally it should be remarked that statistical tensors $\rho_q^2(I_i)$ and $\rho_q^4(I_i)$ for even q, are unaffected by the transformation $A \to -A$. However, this is not the case for $P \to -P$, which leads to changes in both signs and numerical values. Thus, in preparing tables of statistical tensors, it is necessary to consider the two combinations $(\pm A, P)$ and $(\pm A, -P)$. This is easily achieved by allowing W to take on positive values $(+A, +P)$ and negative values $(-A, -P)$, respectively.

V. TRANSFORMATIONS OF STATISTICAL TENSORS UNDER SPATIAL ROTATIONS OF $\theta = \frac{1}{2}\pi$ IN THE z-x AND z-y PLANES, RESPECTIVELY

It has already been remarked that the accompanying tables of statistical tensors have been calculated with respect to the frame of reference defined by Fig. 1(a). However in certain situations, it may be preferable to work with statistical tensors, defined with respect to other frames of reference, such as those shown in Figs. 1(b) and 1(c). For example, if the quadrupole interaction is much stronger than that of the Zeeman interaction, then the co-ordinate system defined by Fig. 1(b), may be more appropriate. Such transformations are easily effected using Eq. (7). For $\lambda = 2$ and 4 we find

$$\begin{pmatrix} \rho_2^2 \\ \rho_0^2 \\ \rho_{-2}^2 \end{pmatrix}_b = \begin{pmatrix} \frac{1}{4} & \frac{1}{2}(\frac{3}{2})^{1/2} & \frac{1}{4} \\ \frac{1}{2}(\frac{3}{2})^{1/2} & -\frac{1}{2} & \frac{1}{2}(\frac{3}{2})^{1/2} \\ \frac{1}{4} & \frac{1}{2}(\frac{3}{2})^{1/2} & \frac{1}{4} \end{pmatrix} \begin{pmatrix} \rho_2^2 \\ \rho_0^2 \\ \rho_{-2}^2 \end{pmatrix}_a \tag{23}$$

and

$$\begin{pmatrix} \rho_4^4 \\ \rho_2^4 \\ \rho_0^4 \\ \rho_{-2}^4 \\ \rho_{-4}^4 \end{pmatrix}_b = \begin{pmatrix} \frac{1}{16} & \frac{(7)^{1/2}}{8} & \frac{1}{8}(\frac{35}{2})^{1/2} & \frac{(7)^{1/2}}{8} & \frac{1}{16} \\ \frac{(7)^{1/2}}{8} & \frac{1}{4} & -\frac{1}{4}(\frac{5}{2})^{1/2} & \frac{1}{4} & \frac{(7)^{1/2}}{8} \\ \frac{1}{8}(\frac{35}{2})^{1/2} & -\frac{1}{4}(\frac{5}{2})^{1/2} & \frac{3}{8} & -\frac{1}{4}(\frac{5}{2})^{1/2} & \frac{1}{8}(\frac{35}{2})^{1/2} \\ \frac{(7)^{1/2}}{8} & \frac{1}{4} & -\frac{1}{4}(\frac{5}{2})^{1/2} & \frac{1}{4} & \frac{(7)^{1/2}}{8} \\ \frac{1}{16} & \frac{(7)^{1/2}}{8} & \frac{1}{8}(\frac{35}{2})^{1/2} & \frac{(7)^{1/2}}{8} & \frac{1}{16} \end{pmatrix} \begin{pmatrix} \rho_4^4 \\ \rho_2^4 \\ \rho_0^4 \\ \rho_{-2}^4 \\ \rho_{-4}^4 \end{pmatrix}_a , \tag{24}$$

which can be further simplified, on noting that we have $\rho_2^2 \equiv \rho_{-2}^2$, $\rho_2^4 \equiv \rho_{-2}^4$, and $\rho_4^4 \equiv \rho_{-4}^4$, for the Hamiltonian of Eq. (1).

For pure quadrupole alignment $(x=0)$ only $(\rho_0^2)_b$ and $(\rho_0^4)_b$ are nonzero, with respect to the frame of reference of Fig. 1(b). This observation, together with Eqs. (23) and (24), can be used therefore to show that

$$\left[\frac{\rho_2^2(x=0)}{\rho_0^2(x=0)}\right]_a = -(\tfrac{3}{2})^{1/2} , \tag{25}$$

$$\left[\frac{\rho_2^4(x=0)}{\rho_0^4(x=0)}\right]_a = -\tfrac{1}{3}\, 10^{1/2} \tag{26}$$

and

$$\left[\frac{\rho_4^4(x=0)}{\rho_0^4(x=0)}\right]_a = +\tfrac{1}{3}\,(\tfrac{35}{2})^{1/2} , \tag{27}$$

which provides a useful symmetry check on the tabulations for $x=0$. For the pure magnetic case $(x=1.0)$, the calculated values have been compared with the earlier tabulations of Krane.[8] However for general x it is not possible to devise symmetry tests, other than the simple transformations $A \to -A$ and $P \to -P$.

Finally, we observe that the matrices required to transform the $(\rho_q^\lambda)_a$ into the $(\rho_q^\lambda)_c$ of Fig. 1(c), may be derived from those of Eqs. (23) and (24), on multiplying each matrix element by $(-)^{(m+m_1)/2}$. For example we have

$$\begin{pmatrix} \rho_2^2 \\ \rho_0^2 \\ \rho_{-2}^2 \end{pmatrix}_c = \begin{pmatrix} \frac{1}{4} & -\frac{1}{2}(\frac{3}{2})^{1/2} & \frac{1}{4} \\ -\frac{1}{2}(\frac{3}{2})^{1/2} & -\frac{1}{2} & -\frac{1}{2}(\frac{3}{2})^{1/2} \\ \frac{1}{4} & -\frac{1}{2}(\frac{3}{2})^{1/2} & \frac{1}{4} \end{pmatrix} \begin{pmatrix} \rho_2^2 \\ \rho_0^2 \\ \rho_{-2}^2 \end{pmatrix}_a . \tag{28}$$

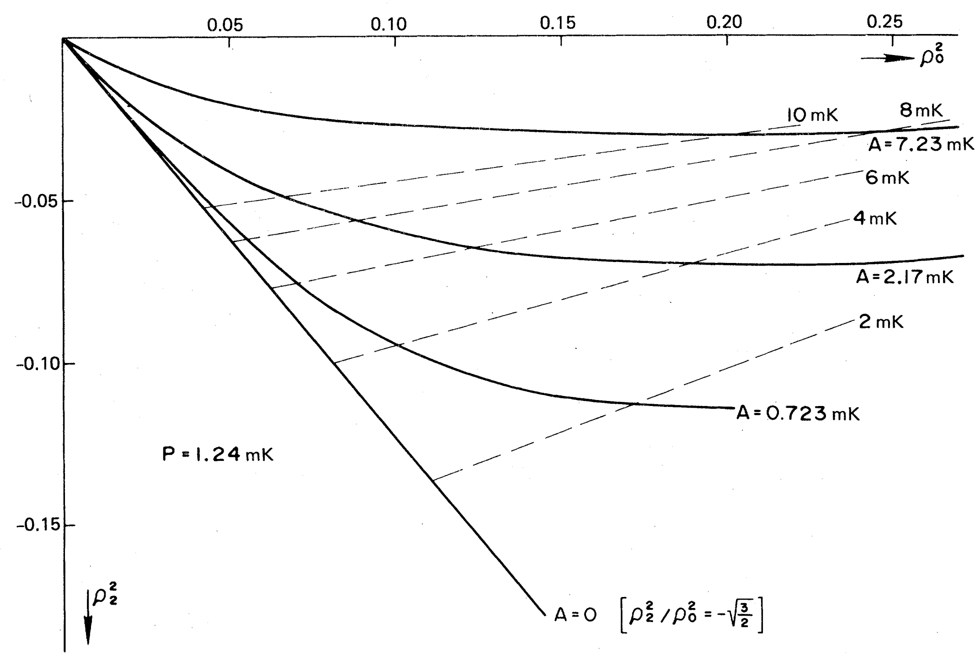

FIG. 2. Statistical-tensor diagram of ρ_2^2 vs ρ_0^2 for a fixed value of the quadrupole parameter $P=1.23$ mK and various magnetic hyperfine fields. (Ref. 9). The dashed lines are isotherms.

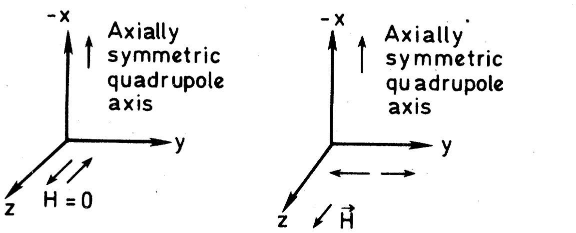

FIG. 3. Spin-flop transition in a nuclear antiferromagnet induced by a small applied field $\vec{H}$.

VI. STATISTICAL-TENSOR DIAGRAMS

It is often convenient when analyzing the results of a particular nuclear-orientation experiment, using Eqs. (9) and (10), to present the results in the form of ρ_2^2 vs ρ_0^2, etc., diagrams. Such an example is shown in Fig. 2 for the particular case of a known fixed quadrupole parameter P and various magnetic hyperfine fields. The dotted lines are isotherms and such plots can be used, for example, to determine both the nuclear hyperfine parameter A and the nuclear-spin temperature T.

These diagrams are also useful in the identification of either nuclear-spin reorientations or nuclear spin-flop transitions. As an example, consider a nuclear ensemble which orders antiferromagnetically, with the spins directed along the z axis as shown in Fig. 3(a). For simplicity we set the quadrupole parameter $P \equiv 0$, so that the ensemble is characterized by a positive definite $(\rho_0^2)_i$ and a vanishing $(\rho_2^2)_i$. If the application of a small applied field along the z axis now induces the spin-flop transition, shown in Fig. 3(b), then abrupt changes in both the sign and magnitude of ρ_0^2 and ρ_2^2 can be anticipated. The situation is summarized in Fig. 4, which has been prepared with the aid of the transformation tables of Sec. V. Following the spin-flop transition, the new statistical tensors are related to those of the initial frame of reference Fig. 1(a), via the equations

$$\rho_0^2 = -\tfrac{1}{2}(\rho_0^2)_i \tag{29}$$

and

$$\rho_2^2 = -\tfrac{1}{2}(\tfrac{3}{2})^{1/2}(\rho_0^2)_i \tag{30}$$

provided the intrinsic nuclear polarization is un-

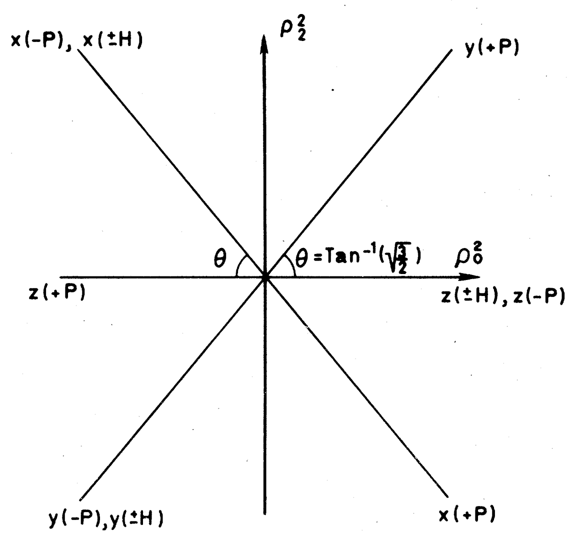

FIG. 4. Statistical-tensor diagrams of ρ_0^2 vs ρ_2^2 for either pure magnetic or pure quadrupole interactions, directed along various principal axes. $x(H), y(H), z(H)$ denote a pure magnetic hyperfine field directed along the x,y,z axes, respectively. $x(P), y(P), z(P)$ denote a pure axially symmetric quadrupole interaction directed along the x,y,z axes, respectively.

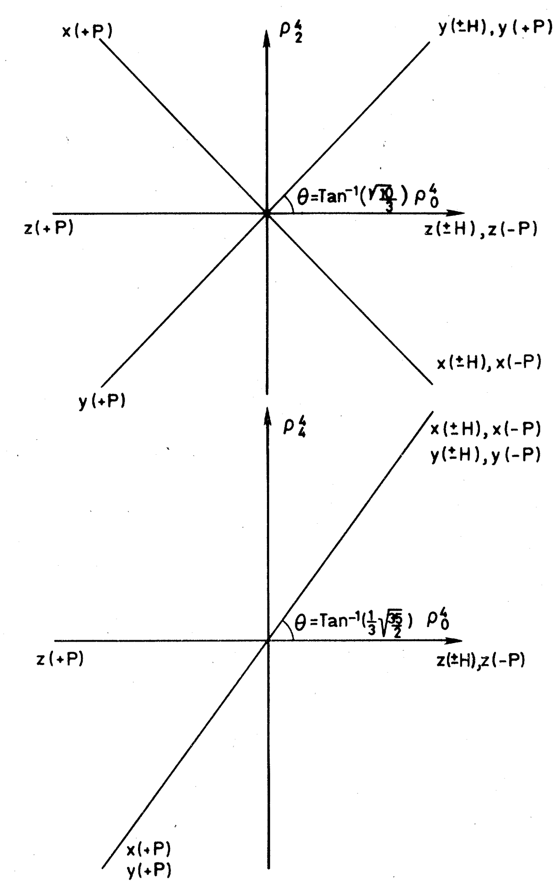

FIG. 5. Statistical-tensor diagrams of ρ_2^4 vs ρ_0^4 and ρ_4^4 vs ρ_0^4 for either pure magnetic or pure quadrupole interactions, directed along various principal axes. (See Fig. 4.)

changed. Such techniques have recently been used (Stone *et al.*[9]) in an attempt to identify a spin-flop transition, in the Van Vleck enhanced nuclear antiferromagnetic $HoVO_4$.

Finally, in Fig. 5, we show similar diagrams for the statistical tensors ρ_0^4, ρ_2^4, and ρ_4^4. These are best presented in the form of two separate two-dimensional plots of ρ_2^4 vs ρ_0^4 and ρ_4^4 vs ρ_0^4. Note that as expected, ρ_4^4 is unable to distinguish between the x and y axes.

ACKNOWLEDGMENTS

The support of the Science Research Council is gratefully acknowledged and I. A. Campbell would like to thank the Science Research Council for the award of a Senior Visiting Fellowship. In addition both G. J. Bowden and I. A. Campbell would like to thank members of the Clarendon Laboratory for their kind hospitality during the course of this work.

*Permanent address: School of Physics, Univ. of New South Wales, Kensington, NSW 2033, Australia.

†Permanent address: Laboratoire de Physique des Solids, Univ. de Paris-Sud, 91405 Orsay, France.

[1]B. N. Samoilov, V. V. Skylarevskii and E. P. Stepanov, Sov. Phys. JETP 9, 972 (1959).

[2]R. M. Steffen and H. Frauenfelder, in *Perturbed Angular Correlations,* edited by E. Karlson, E. Matthias, and K. Siegbahn. (North-Holland, Amsterdam, 1964).

[3]R. M. Steffen and K. Alder, *The Electromagnetic Interaction in Nuclear Spectroscopy* (North-Holland, Amsterdam, 1975), p. 505.

[4]U. Fano, Phys. Rev. 90, 577 (1953).

[5]U. Fano, Rev. Mod. Phys. 29, 76 (1957).

[6]A. R. Edmonds, *Angular Momentum in Quantum Mechanics* (Princeton University, Princeton, N. J., 1960).

[7]See AIP document no. PAPS PRBMDO-20-352-07 for 7 pages of the complete compilation of tables. Order by PAPS number and journal reference from American Institute of Physics, Physics Auxiliary Publication Service, 335 East 45th Street, New York, N.Y. 10017. The price is $1.50 for each microfiche (98 pages), or $5 for photocopies of up to 30 pages with $0.15 for each additional page over 30 pages. Airmail additional. Make checks payable to the American Institute of Physics. This material also appears in *Current Physics Microform,* the monthly microfilm edition of the complete set of journals published by AIP, on the frames immediately following this journal article.

[8]K. S. Krane, Tables of Coefficients for Analysis of Angular Distribution of Gamma Radiation from Oriented Nuclei, LASL Report LA 4677, 1971 (unpublished).

[9]Stone *et al.* (unpublished).